


# Long-Term Exposure of Fresh and Aged Nano Zinc Oxide Promotes Hepatocellular Carcinoma Malignancy by Up-Regulating Claudin-2

Na Yu<sup>1,\*</sup>, Mingqin Su<sup>1,\*</sup>, Juan Wang<sup>2</sup>, Yakun Liu<sup>1</sup>, Jingya Yang<sup>1</sup>, Jingyi Zhang<sup>1</sup>, Meimei Wang<sup>1</sup> 

<sup>1</sup>Department of Pathophysiology, School of Basic Medical Science, Anhui Medical University, Hefei, 230032, People's Republic of China; <sup>2</sup>Department of Public Health Inspection and Quarantine, School of Public Health, Anhui Medical University, Hefei, 230032, People's Republic of China

\*These authors contributed equally to this work

Correspondence: Meimei Wang, Department of Pathophysiology, School of Basic Medical Science, Anhui Medical University, No. 81, Mei-Shan Road, Hefei, 230032, People's Republic of China, Email wangmm@ustc.edu.cn

**Background:** Tumor development and progression is a long and complex process influenced by a combination of intrinsic (eg, gene mutation) and extrinsic (eg, environmental pollution) factors. As a detoxification organ, the liver plays an important role in human exposure and response to various environmental pollutants including nanomaterials (NMs). Hepatocellular carcinoma (HCC) is one of the most common malignant tumors and remains a serious threat to human health. Whether NMs promote liver cancer progression remains elusive and assessing long-term exposure to subtoxic doses of nanoparticles (NPs) remains a challenge. In this study, we focused on the promotional effects of nano zinc oxide (nZnO) on the malignant progression of human HCC cells HepG2, especially aged nZnO that has undergone physicochemical transformation.

**Methods:** In in vitro experiments, we performed colony forming efficiency, soft agar colony formation, and cell migration/invasion assays on HepG2 cells that had been exposed to a low dose of nZnO (1.5 µg/mL) for 3 or 4 months. In in vivo experiments, we subcutaneously inoculated HepG2 cells that had undergone long-term exposure to nZnO for 4 months into BALB/c athymic nude mice and observed tumor formation. ZnCl<sub>2</sub> was administered to determine the role of zinc ions.

**Results:** Chronic low-dose exposure to nZnO significantly intensified the malignant progression of HCC cells, whereas aged nZnO may exacerbate the severity of malignant progression. Furthermore, through transcriptome sequencing analysis and in vitro cellular rescue experiments, we demonstrated that the mechanism of nZnO-induced malignant progression of HCC could be linked to the activation of Claudin-2 (CLDN2), one of the components of cellular tight junctions, and the dysregulation of its downstream signaling pathways.

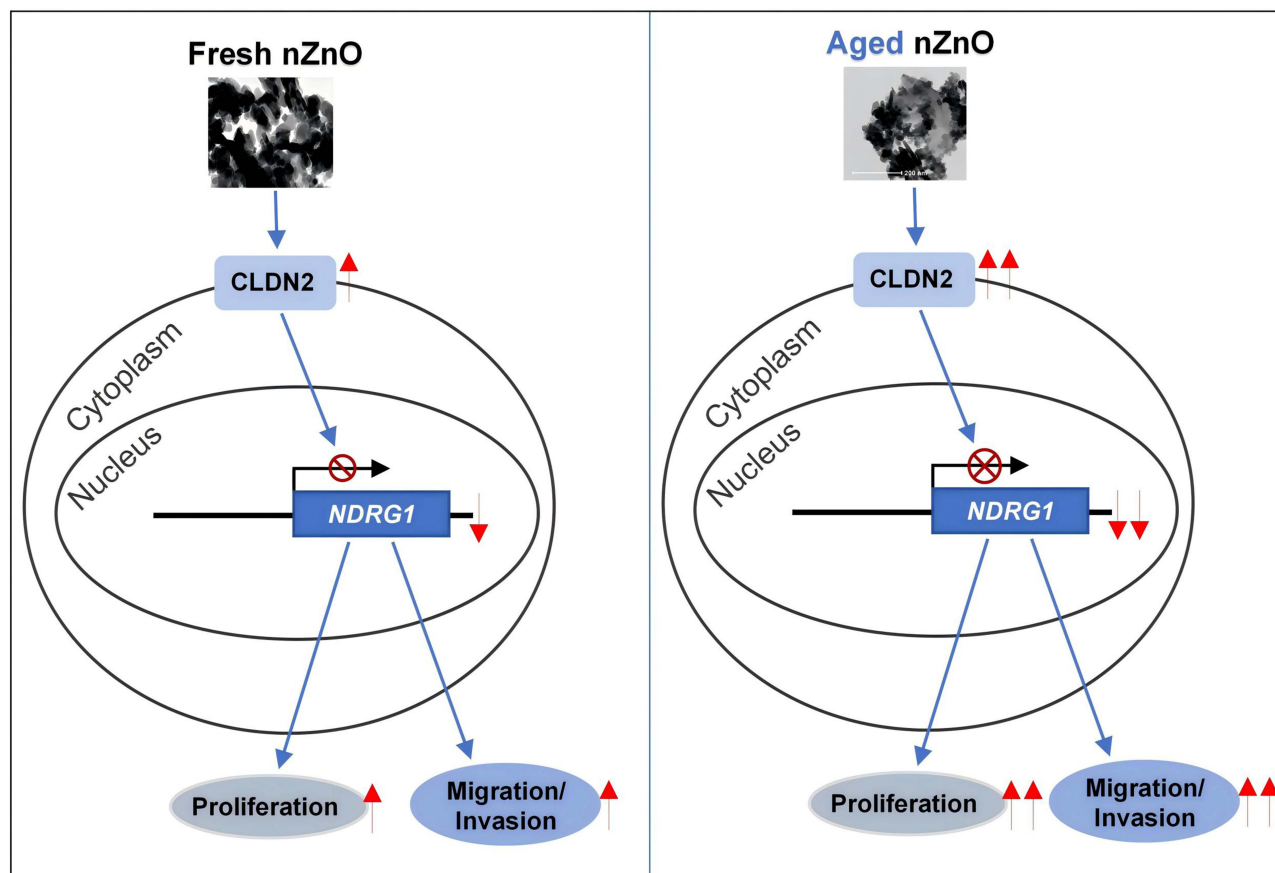
**Conclusion:** Long-term exposure of fresh and aged nZnO promotes hepatocellular carcinoma malignancy by up-regulating CLDN2. The implications of this work can be profound for cancer patients, as the use of various nanoproducts and unintentional exposure to environmentally transformed NMs may unknowingly hasten the progression of their cancers.

**Keywords:** nano zinc oxide, environmental transformation of NPs, long-term exposure, malignant progression of tumors, CLDN2

## Introduction

The incidence and mortality of tumors have always been high worldwide, and the infiltration and metastasis of tumor cells accounts for over 90% of cancer-related deaths.<sup>1-3</sup> Of all cancers, liver cancer exacts the fourth highest economic cost because of its high morbidity and mortality.<sup>4</sup> The two kinds of major factors that promote malignant progression of tumors are genetic and environmental factors.<sup>5</sup> Although many researches focus on the genetic factors of cancer, adverse environmental exposures and pollutants play an equally crucial role in cancer initiation and development.<sup>5-7</sup> Omnipresent Nanomaterials (NMs), as a new kind of environmental pollutants, have aroused a widespread concern of its safety issue-biologically and ecologically,<sup>8</sup> but their carcinogenic and cancer-promoting related effects have not been well elucidated so far.

## Graphical Abstract



Nano zinc oxide (nZnO) is one of the earliest commercially produced and most widely used NMs,<sup>9–11</sup> and has been added to many products, such as food, pigments, skin care products, and medical materials.<sup>12,13</sup> This economic success is accompanied by its presence in the environment and the risk of potentially adverse effects on human health.<sup>14,15</sup> In recent years, a large number of studies have confirmed that nZnO can damage the cell membrane system, leading to oxygen stress, endoplasmic reticulum stress, DNA damage, autophagy, apoptosis, and altered expression of related proteins,<sup>16–19</sup> impairing individual animal systems such as the lungs, liver, heart, brain, and reproduction.<sup>10,18</sup> Although respiration, ingestion, and dermal exposure are all ways in which animals and humans are exposed to nZnO, with a gradual understanding of the tissue distribution of nZnO, the liver has been determined as the main target organ for ZnO deposition.<sup>20–26</sup> In an earlier study, 5-week-old Sprague-Dawley rats were orally exposed to different doses (500, 250, and 125 mg/kg) of nZnO for 90 consecutive days, and a dose-dependent increase in Zn concentration in the liver was demonstrated.<sup>27</sup> Another pharmacokinetic study confirmed that the liver of Wistar rats was the site of initial accumulation of nZnO, with the highest level reaching 30 min after treatment, whereas peak accumulation was reached on day 7 in rats exposed to continuous dosing.<sup>28</sup> In addition to its accumulation in the liver, nZnO has been demonstrated to significantly induce hepatic impairment, including genotoxicity, in *in vitro* cells, and human 3D liver microtissue models.<sup>29,30</sup> Later, in *in vivo* experiments, Kong et al<sup>31</sup> demonstrated that oral exposure to nZnO for three months caused anemia and liver damage, affected the antioxidant system, and impacted liver function in mice. To date, there have been many studies on liver injury caused by nZnO, but whether nZnO promotes the progression of hepatocellular carcinoma (HCC) remains unknown. It is worth exploring whether NMs are a class of environmental risk factors that promote invasion and metastasis of HCC, a long-standing problem that threatens human life.

Given that much emphasis has been placed on pristine/fresh NMs that do not enter the environment after synthesis, and the toxicity assessment of transformed/aged NMs has been neglected, we have been very concerned about the environmental and health effects of NMs in the transformed state in order to get closer to the actual situation. nZnO is not as stable as nTiO<sub>2</sub> and carbon nanotubes, which have been classified as class 2B carcinogens<sup>7,32</sup> and have been shown to promote cancer progression as well.<sup>3,33</sup> nZnO is prone to undergo aging processes such as chemical transformation, aggregation, and dissolution owing to the influence of various environmental factors after being intentionally or unintentionally released into the natural environment, such as air and water.<sup>34–37</sup> As a result, what people are actually exposed to are possibly to be the transformed NMs with properties, states, and toxic effects that are different from those of their pristine counterparts.<sup>38,39</sup> Previously, we observed that nZnO underwent drastic chemical changes during aging, and that aged nZnO showed lower cytotoxicity but higher mutagenicity.<sup>40</sup> Later, we demonstrated that aged nZnO (as compared to fresh counterparts) induced higher carcinogenicity in wild-type mouse embryonic fibroblast (MEF SHP2<sup>+/+</sup>) cells and isogenic cytoplasmic protein tyrosine phosphatase (SHP2) point mutation (MEF SHP2<sup>D61G/+</sup>) cells, as evidenced by the formation of tumors in BALB/c athymic nude mice.<sup>41</sup> In light of the stronger carcinogenic potential of aged nZnO, we investigated whether aged nZnO at nontoxic concentrations would exhibit stronger pro-cancer progression effects, that is, promote the malignant progression of cancer cells. The dose and duration of exposure to a pollutant that is considered safe for an average healthy person is uncertain as to whether it is still safe for patients with cancer. Given the important role of the liver as a detoxification organ in human exposure to and response to various environmental pollutants, including nanoparticles (NPs),<sup>21,42</sup> we chose the relatively low-metastatic (poor tumorigenicity in nude mice) human hepatocellular carcinoma cell line HepG2 as the experimental subject for chronic exposure to nZnO in vitro. HepG2 cells were exposed to a subtoxic dose (1.5 µg/mL) of fresh or aged nZnO for 16 and 24 weeks, respectively. We examined anchorage-dependent cell growth, migration, and invasion abilities of the cells after exposure for different time periods. We discovered that long-term exposure to low dose of both fresh and aged nZnO promoted the malignant progression of HepG2 cells, including invasive metastatic and pro-tumorigenic abilities in nude mice. Consistent with our hypothesis, aged nZnO showed a stronger ability than fresh NPs to promote cancer cell progression. Delving deeper into the mechanistic study showed that nZnO enhanced HepG2 cell progression, partly by up-regulating Claudin-2 (CLDN2), a well-defined component of cellular tight junctions.<sup>43</sup> Overall, our findings provide new insights into the potential risk that exposure to nZnO may promote cancer progression, highlight the role of low-dose, but long-term exposure, and emphasize the influence of the environment on the transformation of NMs and their biological toxicity.

## Materials and Methods

### Nanoparticles and Characterization of nZnO

Nano ZnO, with an advertised particle size of either 20 nm (99.5% purity, nearly spherical), was obtained from Nanostructured & Amorphous Materials (Houston, TX). Detailed information on the preparation and characterization of nZnO was previously reported by Wang et al.<sup>40</sup> A stock solution (1 mg/mL) of nZnO was prepared in Milli-Q water and dispersed via ultrasonic vibration for 20 min to prevent aggregation. The desired concentrations of nZnO for acute and chronic cellular exposure were freshly prepared by diluting the stock solution with cell culture medium immediately before the experiment. The freshly prepared fresh NPs suspension (referred as fresh) was stored at room temperature (25°C) for naturally aging process to 60 days (referred as aged). After dilution, both fresh and aged nZnO at 100 µg/mL in Milli-Q water was subjected to transmission electron microscopy TEM (JEOL, JEM-2010) and scanning electron microscopy SEM (GeminiSEM 300, ZEISS, Germany) at the Center for Scientific Research of Anhui Medical University to confirm the particle size and determine the differences in the morphologies of the fresh and aged NPs. The hydrodynamic size and zeta potential parameters of NPs dispersions (100 µg/mL in distilled water or Dulbecco's modified Eagle's medium) were analyzed in triplicate by dynamic light scattering (DLS) using a Zetasizer Nano ZSE (Malvern Instruments, UK) by dynamic light scattering (DLS). The soluble fractions (Zn ions) of the NP suspensions were determined by inductively coupled plasma optical emission spectrometry (ICP-OES, EXPEC-6500D, Focused

Photonics Inc., Hangzhou, China). X-ray diffraction (XRD, PANalytical B. V., Shanghai, China) was performed to identify the crystalline phase changes between fresh and aged NPs.

## Short-Term Exposure and Cell Viability

HepG2 cells were obtained from the China Center for Type Culture Collection (Shanghai, China) and were cultured in the Dulbecco's modified Eagle's medium (DMEM) supplemented with 10% fetal bovine serum (FBS, Gibco, Grand Island, NY, USA) and 1% penicillin-streptomycin at 37 °C in a humidified 5% CO<sub>2</sub>/95% air incubator and passaged. To ensure proper dispersion of NPs, the stock suspensions were vortexed and sonicated (100 W) for 30 min before taking aliquots to prepare working solutions (in the medium DMEM/10% FBS). The working solutions were sonicated for 15s before being dispersed in cell culture plates for further cellular assays. HepG2 cells ( $4 \times 10^4$  cells/well) were plated in 12-well plates in triplicate and incubated for 24 h. The cells were then treated with different concentrations of nZnO ranging from 1 to 50 µg/mL in complete medium for 72 h. Cell viability was determined using the Beckman Coulter (Brea, CA, USA) method with a Count star. The plastic culture microplates and flasks used in the experiment were purchased from Corning Incorporated (Corning, NY, USA).

## Quantitative Measurement of Cellular Uptake of Nanoparticles After Acute Exposure by ICP-OES

Cellular uptake of nZnO was quantified using inductively coupled plasma optical emission spectrometry (ICP-OES) after long-term exposure to fresh and aged nZnO. HepG2 cells exposed to 15 µg/mL fresh or aged nZnO for 72 h were washed, harvested, and counted. Then, the cell suspension with  $1 \times 10^7$  cells were added to a test tube with 1.5 mL of HNO<sub>3</sub> (GR), followed by heating at 60 to 70 °C about 2 h until white crystals appeared. The crystals were dissolved in 1.5 mL ultrapure water and quantitatively measured using ICP-OES (EXPEC-6500D, Focused Photonics Inc., Hangzhou, China). The same number of cells without NMs treatment was used as an internal standard. The concentration of Zn in the cells was calculated in picograms per cell.

## Long-Term Exposure

A brief experimental plan including the selected concentrations and times of the whole study was designed, keeping in mind the approach for the NPs toxicity study, as suggested in our previous report,<sup>41</sup> (Figure S1). The final selected exposure concentration was 1.5 µg/mL corresponding to the non-cytotoxic concentration. HepG2 cells were continuously exposed to fresh or aged NPs for 12 weeks (Passage 30th, P30) and 16 weeks (Passage 40th, P40). Approximately  $1 \times 10^5$  cells were seeded in 60 mm dishes and incubated overnight. Every three days, the cells were washed twice with PBS, and fresh medium containing nZnO was added. Unexposed cells were maintained throughout the complete duration of exposure period and were used as controls. Working solutions of nZnO were sonicated for 30 min at 100 W and room temperature. In all cases, nZnO-exposed cells were compared to unexposed passage-matched controls. Subsequently, the malignant biological behavior was verified in in vivo and in vitro experiments.

## Colony Forming Efficiency Assay

Briefly, after 12 and 16 weeks of exposure, normal HepG2 cells or CLDN2-knockdown HepG2 cells were harvested by trypsinization and reseeded at a density of 500 cells/well in 6-well plates. The medium was changed every 4 days. After culturing for two weeks, the colonies were fixed in 4% paraformaldehyde, washed with PBS, and then stained with crystal violet dye (Beyotime, Shanghai, China). The plates were then washed several times with PBS, dried, and photographed. The colonies (> 50 cells) were counted manually.

## Soft-Agar Colony Formation Assay

Anchorage-independent cell growth was assessed using soft agar colony formation assay. After 12 and 16 weeks of exposure, P30 and P40 cells were harvested, resuspended in cell medium, and counted. A layer of 1.2% agarose-containing medium was spread on the bottom of a 6-well plate, and the cell suspension diluted with complete medium



(20% FBS) and 0.6% agarose was mixed in equal proportions and added to the top layer (1000 cells per well). The plates were incubated at 37°C and 5% CO<sub>2</sub> for two weeks. The cell colonies were counted and photographed using a microscope (Carl Zeiss). All experiments were performed at least three times in triplicate.

## Cell Migration and Invasion Assays

Boyden chambers containing 12-well transwell plates (Corning, USA) with polycarbonate filters of 8 µm pore size were used to evaluate the migration and invasion ability. The chambers used for the invasion assay were coated with matrigel (Corning Biocoat, NY, USA).  $5 \times 10^4$  cells under NPs treatment with or without CLDN2 knockdown in 200 µL serum-free DMEM medium were seeded into the upper transwell chamber, and the lower chamber was filled with 700 µL DMEM with 10% FBS to induce chemotaxis. After incubation for 48 h, the cells in the lower chambers were fixed with methylalcohol and stained with 0.1% crystal violet. Finally, the migrated and invaded cells were counted and the images were photographed under a microscope (Nikon ECLIPSE TS100) at 100 × magnification. Five random microscopic fields were counted manually in each well. Data were obtained from triplicate wells.

## In vivo Tumorigenicity Assay

To evaluate whether long-term exposure to low-dose fresh and aged nZnO enhanced tumor growth in vivo, P40 or control cells ( $4 \times 10^6$  cells diluted in 100 µL of PBS) were subcutaneously inoculated into the right underarm of 5-week-old BALB/c athymic nude mice (n = 5). Tumor size was measured using a Vernier caliper. Tumor volume was determined using the formula  $0.24 \times ab^2$ , where  $a$  is the diameter of the base of the tumor and  $b$  is the corresponding perpendicular value. Tumor growth was monitored and recorded daily. The mice were euthanized on day 10 to strip xenograft tumors. The weights of the xenograft tumors were measured. All mice were purchased from Nanjing University Model Animal Research Center (Nanjing, China). All mice were housed in the SPF animal laboratory on a 12 h light/dark cycle with free access to water and a normal diet (temperature 20–24 °C and humidity 40–70%). All animal procedures were performed in accordance with the Guidelines for the Care and Use of Laboratory Animals of Anhui Medical University. The animal experimental design was approved by the Animal Ethics Committee of Anhui Medical University (LLSC 20210812).

## RNA-Sequencing and Data Analysis

Total RNA from HepG2 cells was extracted using TRIzol Reagent (Invitrogen). RNA sequence libraries were generated using standard mRNA strand protocols from Illumina and sequenced on a NovaSeq 6000 platform. Samples were sequenced on the platform to obtain image files, which were transformed using the software of the sequencing platform, and the original data in FASTQ format (Raw Data) were generated. The filtered reads were mapped to the reference genome using the HISAT2 v2.0.5. We used HTSeq (0.9.1) statistics to compare the Read Count values for each gene with the original expression of the gene and then used FPKM to standardize the expression. The difference in gene expression was analyzed using DESeq (1.39.0) with the following screening conditions: expression difference multiple  $|\log_2\text{FoldChange}| > 1$ , significant P-value  $< 0.05$ . Simultaneously, we used the R language P heatmap (1.0.8) software package to perform bidirectional clustering analysis of all different genes in the samples. A heatmap was drawn according to the expression levels of the same gene in different samples and the expression patterns of different genes in the same sample, using the Euclidean method to calculate the distance and Complete Linkage method for clustering.

## RNA Isolation and Quantitative Real-Time PCR (qRT-PCR) Analysis

Total RNA was extracted from cells using TRIzol reagent (Invitrogen) and reverse-transcribed with transcriptase (MonScript™, China), according to the manufacturer's instructions. The cDNAs obtained were mixed with SYBR Green Master Mix (MonAmp™ qPCR Mix, China) and target gene-specific primers (Table S1) for qRT-PCR using a StepOnePlus instrument (Applied Biosystems, USA). GAPDH served as an internal control. The reactions were performed in triplicate and normalized to GAPDH mRNA levels using the  $\Delta\Delta C_t$  method.

## Extraction of Proteins and Western Blotting Analysis

The cells were washed with PBS and resuspended in RIPA lysis buffer containing PMSF (100: 1) at 4 °C for 15 min. The supernatants were collected as the total cellular proteins by centrifugation at 4 °C and 12,000 rpm for 20 min and analyzed using the BCA Protein Assay Kit (Beyotime, Shanghai, China). Finally, 20 µg of protein per sample was separated by 10% SDS-PAGE, transferred to PVDF membranes, then blocked with 5% non-fat milk (w/v) for 2 h with gentle shaking, and then incubated with primary antibodies against CLDN2 (1:500 dilution, Santa Cruz Biotechnology, USA) or GAPDH (1:3000 dilution, Servicebio, China) at 4 °C overnight. Subsequently, the membrane was incubated with a secondary antibody (anti-rabbit/mouse IgG, HRP conjugate, 1:7000 dilution; Elabscience, China) and washed several times with TBST. Protein signal intensity was detected using an imaging system (Fisher Varioskan, Thermo, USA). Finally, Protein densitometric analysis was performed using the ImageJ software. Data are depicted as fold differences compared with untreated controls. GAPDH was used as an internal control.

## Cell Transfection

CLDN2 knockdown using short hairpin RNA (shRNA) was performed by Genechem (China). Double-stranded oligonucleotides corresponding to RNA sequences were cloned into the pGV493-RNAi plasmid. The target sequences for human CLDN2 mRNA were as follows: shRNA#1, CAAAGTCAAGAGTGAGTTCAA, and shRNA#2 GCTCTTTACTTGGGCATTATT. The plasmids were transfected into HepG2 (P40) cells (seeded into 6-well plates at a density of  $7 \times 10^5$  cells per well) using Lipo8000™ Transfection Reagent (Beyotime, China) according to the manufacturer's recommended protocols. Forty-eight hours after transfection, protein expression levels of CLDN2 protein were detected by quantitative RT-PCR.

## Statistical Analysis

All experiments were conducted with a minimum of three replications. Values are presented as mean  $\pm$  standard deviation (SD). The Student's *t*-test (unpaired or paired) was used to determine the significance of the differences between the two groups. Analysis of variance (ANOVA) was used to determine the significance of the differences between multiple groups. Statistical significance was set at *p* value < 0.05. All analyses were performed using Microsoft Excel 2021 or GraphPad Prism, version 8.0.2.

## Results and Discussion

### Characterization of Fresh and Aged nZnO

Thorough particle characterization of both fresh and aged NPs in ddH<sub>2</sub>O or cell medium was previously performed, and the results showed that nZnO underwent sophisticated physicochemical transformations with aging, such as the microstructural changes (from relatively regular crystals to partly irregular, amorphous state), the formation of hydrozincite ( $\text{Zn}_5(\text{CO}_3)_2(\text{OH})_6$ ), and the release of free zinc ions.<sup>40</sup> The changes in the morphology and crystallinity were confirmed by TEM and XRD, respectively (Figure 1). In addition, the hydrodynamic size (nm) /Pdl values and soluble Zn fractions of fresh and aged nZnO were determined in both Milli-Q water and DMEM (Table 1). After the solution was diluted in DMEM, the hydrodynamic size of the agglomerates in the suspension decreased significantly (from 3594 nm decreased to 541 nm for fresh NPs and 5565 nm decreased to 378 nm for aged nZnO). This may be attributable to FBS and other components of the cell culture medium, which stabilize the NPs and contribute to their dispersion.<sup>44</sup> Also, we confirmed that the concentrations of dissolved Zn significantly increased for both fresh (with 7.04 µg/mL increased to 18.14 µg/mL) and aged NPs (with 8.66 µg/mL increased to 20.69 µg/mL). Accordingly, the reported biological effects of nZnO may be partly attributed to the release of Zn ions into the culture medium. Our results showed that, accompanied by the transformation of the crystalline phase, the dissolution of both fresh and nZnO was enhanced significantly when diluted in the cell culture medium. Similar to the widely applied nanoAg, nZnO belongs to a class of NMs that are susceptible to physicochemical transformations.<sup>45,46</sup> Sivry et al<sup>47</sup> and Reed et al<sup>48</sup> reported the transformation of nZnO into  $\text{Zn}_5(\text{CO}_3)_2(\text{OH})_6$  and  $\text{ZnCO}_3$ , which is in line with the results of our present and previous studies.<sup>17,40</sup> Engineered NPs in natural systems are subject to a dynamic physical and chemical environment that will drive the particles away from their pristine or “as manufactured” state, toward largely unknown end points and products.<sup>49</sup> Aging, as physical or chemical transformations over time, is essential for understanding the fate of NPs in the environment.<sup>49,50</sup> Here,

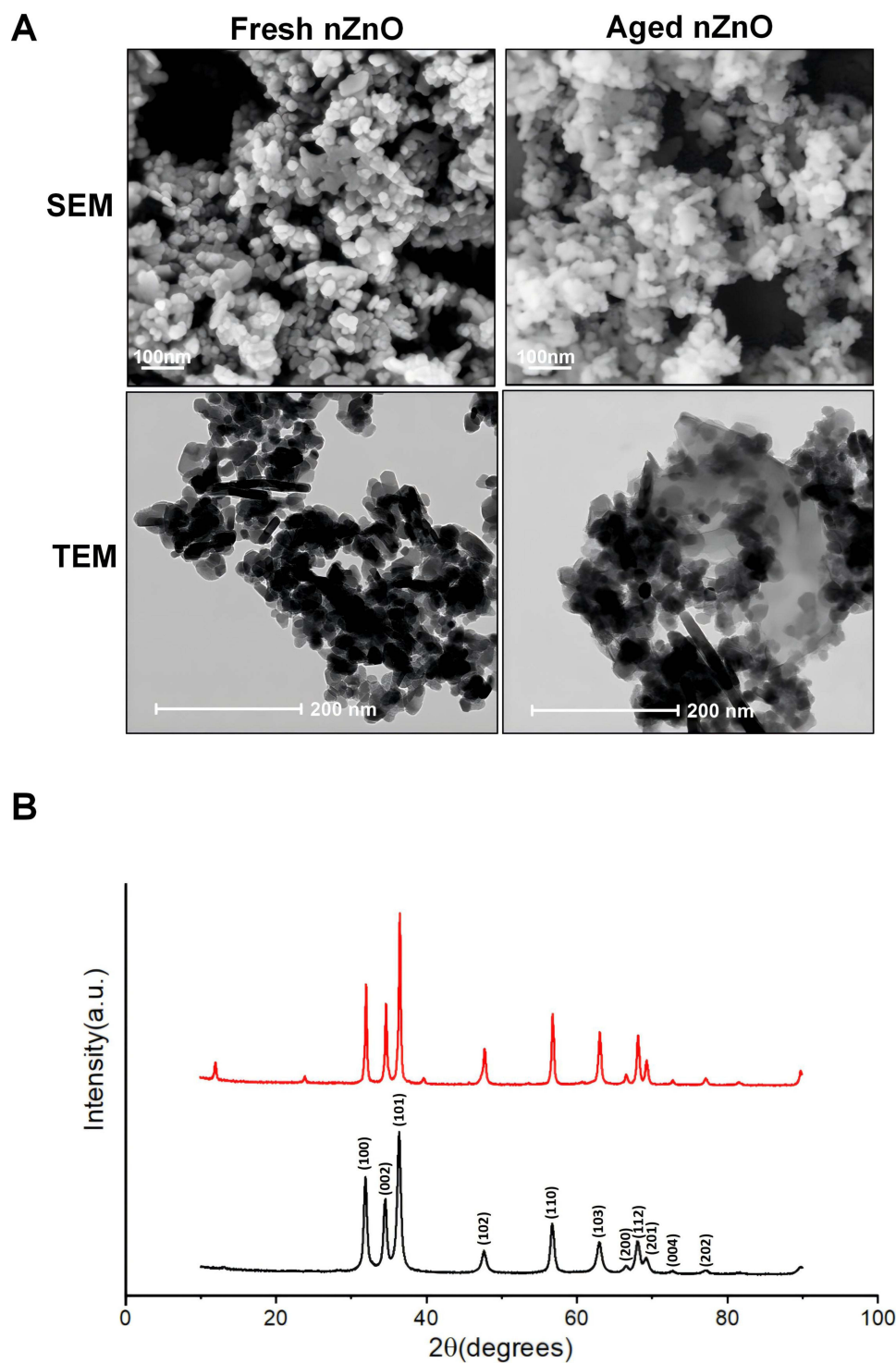


**Figure 1** Characterization of fresh and aged nZnO. (A) SEM and TEM images of fresh and aged nZnO. (B) XRD patterns of fresh (black) and aged (red) nZnO.

ZnO nanopowder was suspended in Milli-Q water (Millipore, 18 M cm) to 1 mg/mL concentration and sterilized by heating to 120 °C for 30 min. The suspension was stored at room temperature for simulating the natural aging process, during which we periodically opened the stock suspension bottles in an ultra-clean bench to give the NMs chances to come into contact with the air ( $\text{CO}_2$ ), a process that we believe is the simplest system for simulating the aging of NMs. Except for our Milli-Q water system, there are studies have shown that nZnO were rapidly transformed to ZnS and  $\text{Zn}_3(\text{PO}_4)_2$  during anaerobic digestion of

**Table 1** Particle Size and Zinc Concentration of Fresh and Aged NP Suspensions. Nanoparticle Size is Expressed as Intensity-Based Average Hydrodynamic Diameter. Bars:  $\pm$ S.D. Pdl = Polydispersity Index. The Dissolved Zn Concentration Was Measured: 50 Mg/mL NPs Were Suspended in Milli-Q Water at Room Temperature or in DMEM/10% FBS at 37 °C for 72 h. The Suspensions Were Centrifuged at 20000Rpm (28 000g) for 1 h, and Then the Zn Concentrations in the Supernatant Were Determined by ICP-OES

nZnO	Milli-Q water				DMEM			
	Hydrodynamic size (nm)	Zeta Potential (mV)	Pdl	Zn Concentration ( $\mu$ g/mL)	Hydrodynamic size (nm)	Zeta Potential (mV)	Pdl	Zn Concentration ( $\mu$ g/mL)
Fresh	3594.17 $\pm$ 207.18	-3.08 $\pm$ 0.64	0.76	7.04 $\pm$ 0.07	541.62 $\pm$ 4.03	-7.63 $\pm$ 0.69	0.65	18.14 $\pm$ 0.17
Aged	5565.00 $\pm$ 551.54	-4.08 $\pm$ 2.34	0.54	8.66 $\pm$ 0.15	378.25 $\pm$ 37.97	-8.45 $\pm$ 0.83	0.60	20.69 $\pm$ 0.18

wastewater and posttreatment processing of sewage sludge.<sup>51,52</sup> In a carbonate-rich water, hydrozincite ( $\text{Zn}_5(\text{CO}_3)_2(\text{OH})_6$ ) and smithsonite ( $\text{ZnCO}_3$ ) were formed by precipitation of zinc ions released by the partial dissolution of nZnO.<sup>47</sup> Different kinds of transformation could readily occur in the environment and in vivo, which greatly affects their properties, behavior, and effects. However, most toxicity, fate, and transport studies to date have used relatively pristine materials, which will behave differently than the transformed ones. While the effects measured for relatively pristine materials may be representative of human exposures occurring at manufacturing or processing sites where direct exposure to relatively pristine NMs is possible, environmental exposures to aquatic organisms and to humans (eg, via inhalation, dermal penetration, drinking water or food ingestion) will be to transformed NMs so data regarding fate and effects of pristine NMs may not be particularly informative. The research community instead needs to focus on understanding the reactivity, fate, mobility, persistence, and effects of the “aged” or transformed NMs where the “aging” process best represents the history of the NM prior to the exposure.<sup>49,53–55</sup>

### Decreased Cancer Cell Viability After Acute Exposure to High Concentrations of Fresh and Aged nZnO

The environmental transformation of NMs indicates that the highly engineered and diverse pristine manufactured NMs are frequently not the type to which organisms are exposed.<sup>38</sup> In our previous studies, we have pointed out that such a transformation may pose the NMs with different or even more serious health risks.<sup>17,40,41</sup> Previously, we unexpectedly found that after natural aging for  $\geq 60$  days, aged (transformed) nZnO induced lower cytotoxicity but higher mutagenicity in human-hamster hybrid ( $A_L$ ) cells<sup>40</sup> and showed stronger tumorigenicity in MEF cells and nude mice.<sup>41</sup> Considering that recent nanotoxicity studies have focused on the health risks to healthy populations and have neglected the effects of nanotoxicity on susceptible populations (eg, those suffering from diseases such as cancer), some researchers have suggested that it is urgent to understand the effects of nanoparticle exposure on these populations. Due to the alterations in physiological structures and functions in susceptible populations, they often suffer more damage from the same exposure.<sup>56</sup> Thus here we used  $\text{ZnCl}_2$  as the zinc ion ( $\text{Zn}^{2+}$ ) control in experiments to investigate the effects of fresh and aged nZnO, as well as  $\text{Zn}^{2+}$  on cancer cell viability. Cell viability is an important index of cytotoxicity, and is defined as the potential of a compound to induce cell death. To understand the effect of nZnO on HepG2 cell proliferation in vitro, we performed colony formation assays. As shown in Figure 2, the viability of HepG2 cells treated with 1, 5, 10, 15, 20, 30, and 50  $\mu$ g/mL nZnO for 72 h decreased in a dose-dependent manner. The exposure dosage and period were selected based on our preliminary studies (data not presented) and similar studies reported in the literature.<sup>19,57,58</sup> Our experimental results showed that acute exposure of HepG2 cells to nZnO resulted in a significant concentration-dependent decrease in cell viability, and therefore, an increase in cytotoxicity compared to the control. The IC50 values of fresh and aged nZnO in HepG2 cells were 15.04 and 21.33  $\mu$ g/mL, respectively. In comparison, fresh nZnO at 10  $\mu$ g/mL began to exhibit pronounced cytotoxicity and 30  $\mu$ g/mL treatment dose gave rise in less than 5% cell viability. Aged nZnO showed lower cytotoxicity than its fresh counterparts, as shown by the higher viability of HepG2 cells at equivalent concentrations and about 12.5% remaining viability of HepG2 cells at 30  $\mu$ g/mL treatment dose. Our current acute cytotoxicity results agreed with those of our previous studies<sup>17,40</sup> and Zhang et al,<sup>59</sup> who studied the contribution of physicochemical

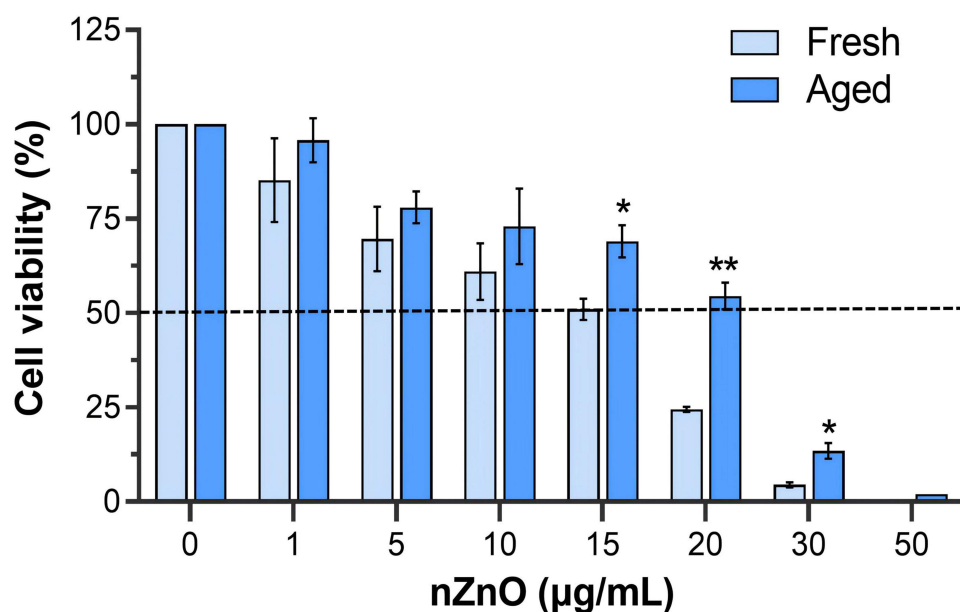


**Figure 2** Acute exposure to nZnO induced cytotoxicity in HepG2 cells. Cells were treated with concentrations ranging from 0 to 50 µg/mL of fresh or aged nZnO for 72 h. Data are represented as mean ± SD (n ≥ 3). \*p < 0.05 versus Fresh group, \*\*p < 0.01 versus Fresh group.

transformations to the toxicity of aged nZnO to *Chlorella vulgaris* and reported the highest toxicity of 30 day-aged nZnO compared to fresh nZnO. Consistent with the cellular viability assay, our ICP-OES data revealed a significant increase in the amount of zinc in nZnO-treated cells compared to the control groups, especially in the aged nZnO group ( $1.57 \times 10^{-13}$  g per cell for fresh NPs vs  $2.03 \times 10^{-13}$  g per cell for aged NPs) (Table S2). The role of dissolution in the toxicity of nZnO has been studied in vitro and in vivo.<sup>60–62</sup> However, partly because the dissolution of nZnO is a complex process, even in deionized water, no consensus has been reached on whether  $\text{Zn}^{2+}$  is a major contributor to the toxicity of nZnO. Some studies have reported that dissolved  $\text{Zn}^{2+}$  ions induce more pronounced toxicity in cells than the NP fractions.<sup>63–65</sup> In contrast, the whole suspension of nZnO instead of the suspension supernatant inhibited the growth of microorganisms, indicating that the toxic effects were mainly attributed to nZnO rather than to the dissolved  $\text{Zn}^{2+}$ .<sup>66,67</sup> Our present and previous studies regarding the cytotoxicity nZnO in vitro suggested that the higher cytotoxicity of fresh nZnO could be mainly due to the intrinsic toxicity of nZnO, while the higher mutagenic potential of aged nZnO might be attributed to the main contribution of  $\text{Zn}^{2+}$  and the lesser contribution from the major transformed products, ie  $\text{Zn}_5(\text{CO}_3)_2(\text{OH})_6$ .<sup>40</sup>

## Enhanced Cancer Cell Proliferation After Chronic Exposure to Low Dose of nZnO

Most studies on NP-induced health risks are short-term focused; however, the wide variety of uses of NPs and their growing release into the environment translate into many ways of human exposure, making it necessary to analyze the long-term effects associated with these materials. In this direction, we examined the long-term promotional effects of nZnO on several oncogenic markers, including proliferation, anchorage-independent cell growth, migration, and invasion potential. First, cancer cell proliferation was assessed by treating HepG2 cells with 1.5 µg/mL fresh nZnO, aged nZnO, or  $\text{ZnCl}_2$  for months. In the colony formation assay, we observed a significantly increased number of colonies in fresh nZnO- and  $\text{ZnCl}_2$ - treated cells, whereas aged nZnO treatments led to a greater increase in colony-forming ability (1.24 folds and 1.7 folds for 30 and 40 passages, respectively, when compared to control groups) (Figure 3). Increasing evidence indicates the transforming ability of different NPs, strengthening the idea that further studies are necessary to unravel the potential long-term effects of NPs and their possible mechanisms of action. For instance,  $\text{TiO}_2$  has been shown to induce anchorage-independent growth of HEK293 and NIH/3T3 cells after 3 weeks;<sup>63</sup> low doses of multi-walled carbon nanotubes show transforming potential of lung epithelial BEAS-2B cells after 4 weeks of exposure;<sup>68</sup> and a 6-week exposure to subtoxic doses of silver NP is sufficient to generate a transformed phenotype in the colon model Caco-2 cells.<sup>69</sup> In the particular case of nZnO, our previous study showed that both fresh and aged nZnO induced the



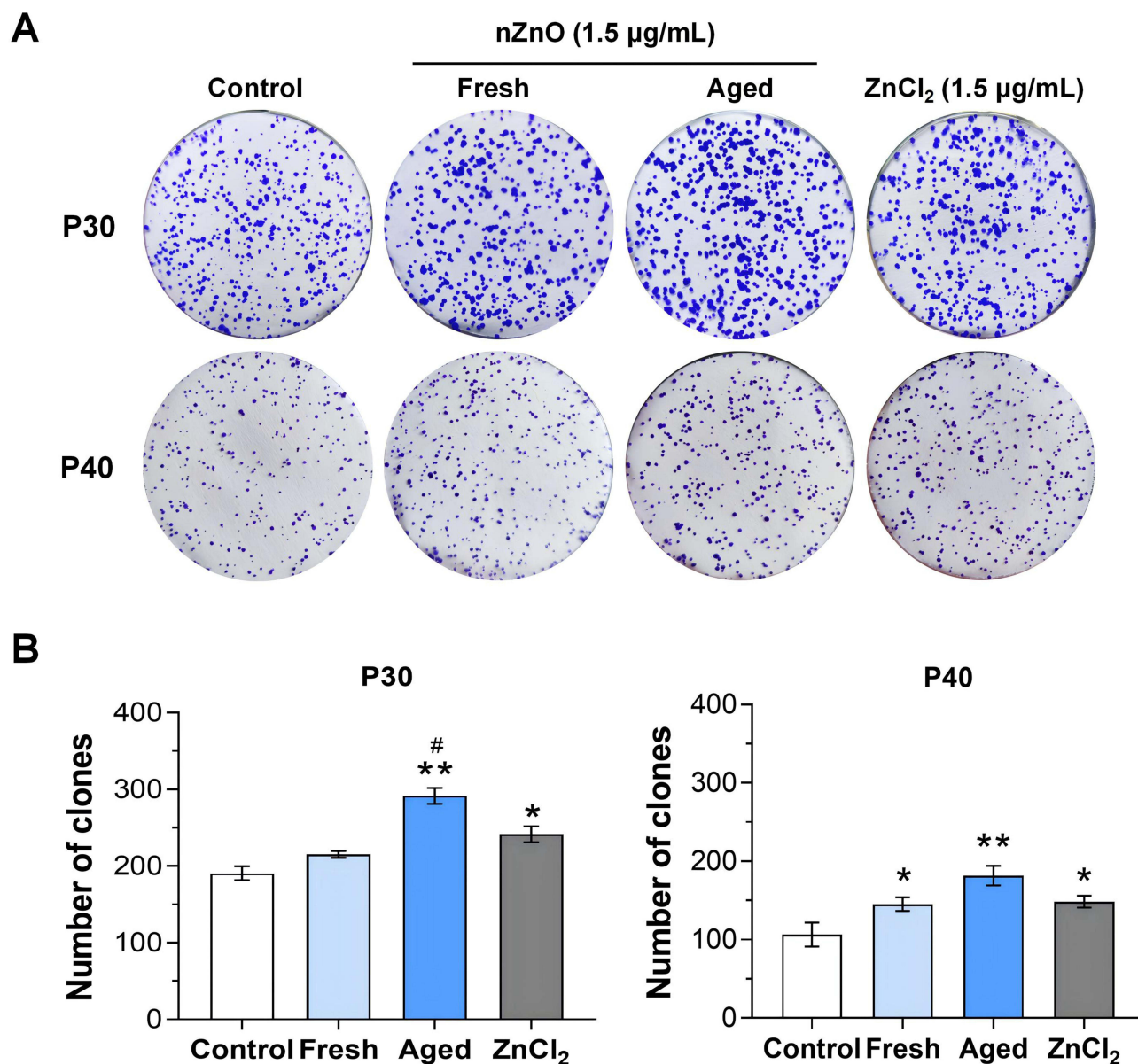


**Figure 3** Long-term exposure to low dose of nZnO increased the proliferation of HepG2 cells. Representative images (**A**) and the statistical analysis result (**B**) of colony forming efficiency assay on HepG2 cells treated with NPs or ZnCl<sub>2</sub>. Data are represented as mean ± SD (n ≥ 3). \*p < 0.05, \*\*p < 0.01 vs Control group, #p < 0.05 vs Fresh group.

malignant proliferation of MEF cells after chronic exposure at sub-toxic doses.<sup>41</sup> In addition, we demonstrated the importance of oxidative DNA damage produced by nZnO and its relationship with the cell transformation process,<sup>17</sup> which is in line with the studies conducted by Annangi et al<sup>70</sup> and Barguilla et al<sup>12</sup>

## Enhanced Soft Agar Colony Formation Abilities of HepG2 Cells After Chronic Exposure to Low Dose of nZnO

In light of the higher carcinogenicity of aged nZnO that we discovered earlier,<sup>41</sup> and the above results regarding the enhancement effects of nZnO on HepG2 proliferation, we further investigated whether aged nZnO would also show a stronger ability to promote cancer cell progression. Anchorage-independent growth is an important hallmark of cell transformation. Therefore, we examined the ability of long-term exposure to HepG2 cells to form colonies on soft agar. As shown in Figure 4, 12 weeks (30 passages) of exposure to aged nZnO at 1.5 µg/mL were enough to cause a significant increase

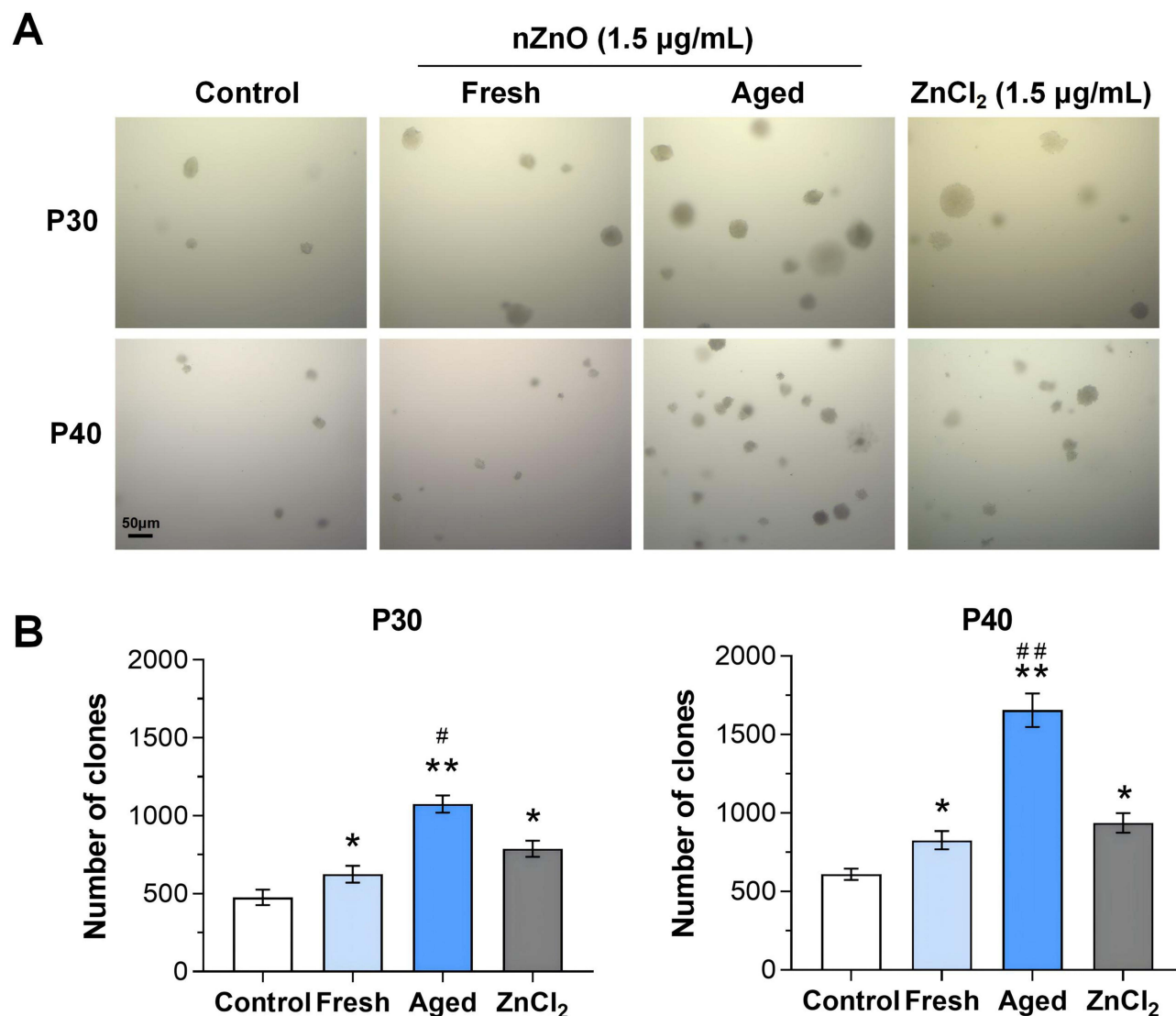


**Figure 4** Long-term exposure to low dose of nZnO increased the soft agar colony formation ability of HepG2 cells. Representative images (A) and the statistical analysis result (B) of the soft agar colony formation assay on HepG2 cells treated with NPs or ZnCl<sub>2</sub>. Data are represented as mean ± SD (n ≥ 3). \*p < 0.05, \*\*p < 0.01 vs Control group, #p < 0.05, ##p < 0.01 vs Fresh group.

in the number of colonies (2.26 folds and 1.72 folds when compared to control and fresh groups, respectively), let alone an extension of the exposure time to 16 weeks (40 passages), when the ability to form clones was even greater (2.71 folds and 2.0 folds when compared to Control and Fresh groups, respectively). The results indicated that compared with the fresh nZnO and ZnCl<sub>2</sub> exposure groups, aged nZnO-exposed cancer cells showed severe signs of malignant progression. This observation is in line with a previous study on MEFs<sup>41</sup> and other studies that reported that nZnO, independent of their size, was able to promote anchorage-independent growth in soft agar in both HEK293 and NIH/3T3 cells.<sup>63</sup> However, Annangi et al<sup>70</sup> reported negative results on soft agar colony formation ability in both wild-type MEF and their isogenic 8-oxo-guanine DNA glycosylase 1 (*Ogg1*) knockout cells after 12 weeks of treatment with 1 µg/mL nZnO. This conflict might be attributed to the use of different cell lines, particularly different exposure doses and time ranges, or different characteristics of the NPs themselves.

## Enhanced Migration and Invasion Abilities of HepG2 Cells After Chronic Exposure to Low Dose of nZnO

Tumor cell migration and invasion are prerequisites for tumor metastasis, enabling cells to break through the vascular endothelial cells into the blood circulation.<sup>71</sup> Therefore, in this study, the effect of nZnO on HepG2 cell migration and

invasion was evaluated using a transwell assay to further confirm our aforementioned data obtained in the soft agar colony formation assay. As shown in Figure 5, HepG2 cells treated with 1.5 µg/mL fresh nZnO, aged nZnO, or ZnCl<sub>2</sub> for 12 weeks showed increased migration ability. Aged nZnO showed the most striking effect (2.46-fold), followed by ZnCl<sub>2</sub> (1.78-fold) and fresh nZnO (1.45-fold). Prolonged exposure (16 weeks) resulted in a more pronounced elevation in the migration ability, and the increasing trend was comparable to that observed in the 12 week-treatment groups. In parallel, increased invasion abilities of HepG2 cells were found in all treatment groups, which were 152% (aged nZnO, 12 weeks), 64.0% (ZnCl<sub>2</sub>, 12 weeks), and 33.2% (fresh nZnO, 12 weeks) higher than control group, respectively. Similar to that observed in the migration assay, 16 weeks-treatment appears to have a stronger effect on cell invasion (Figure 6). There is a growing body of evidence showing that fresh nZnO can promote cell proliferation and migration as well as independent anchoring growth and angiogenesis, all of which are hallmarks of tumorigenesis.<sup>9,63</sup> However, studies on whether aged nZnO can promote the malignant progression of cancer cells have not been reported. The novelty of our current study is that we focused on aged nZnO and its promotional effects on cancer cell progression. Another issue that must be addressed is the role of Zn<sup>2+</sup>. It has been reported that nZnO can liberate free Zn<sup>2+</sup> in acidic

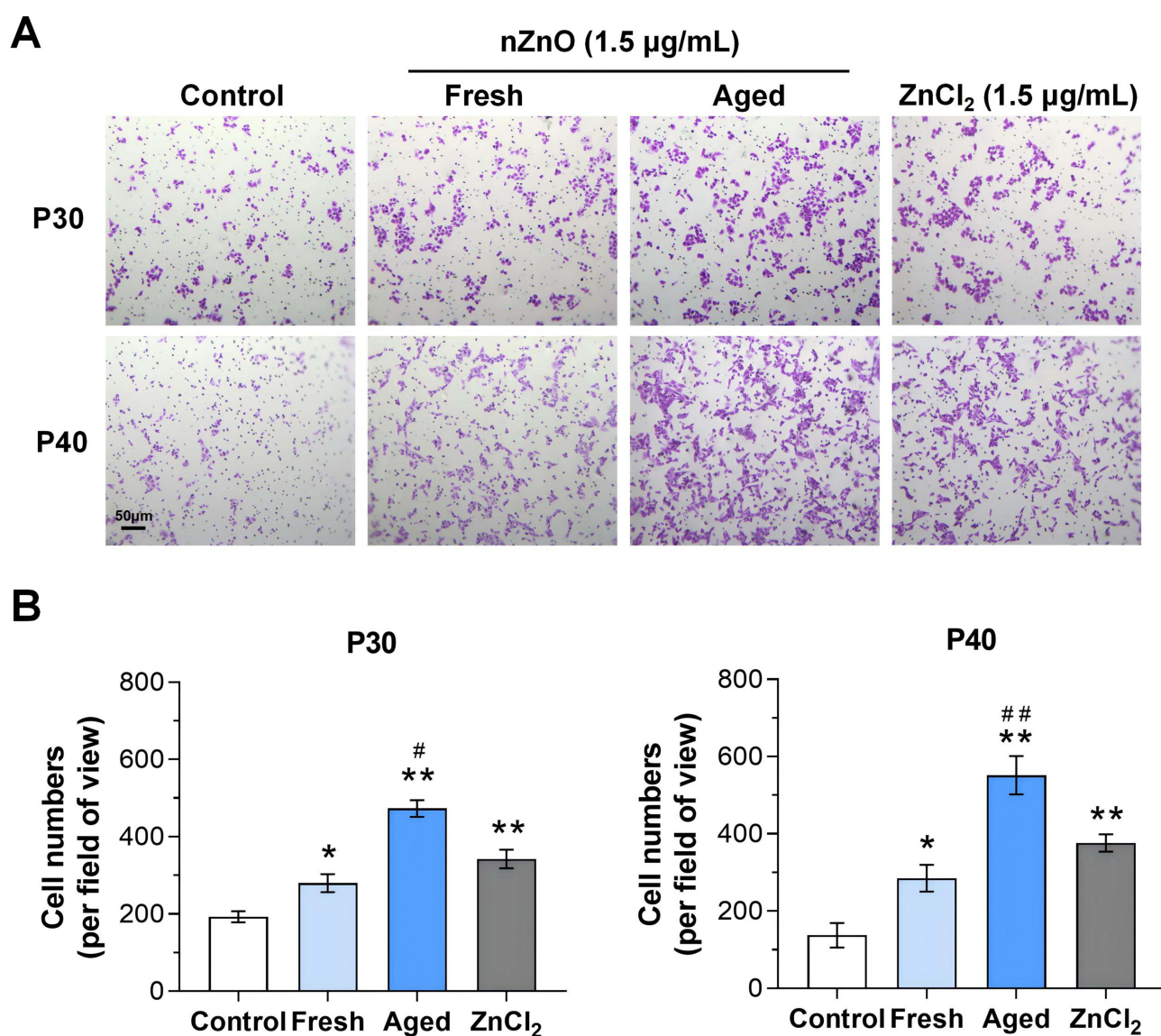


**Figure 5** Long-term exposure to low dose of nZnO increased the migration abilities of HepG2 cells. Representative images (A) and the numbers (B) of HepG2 cells that passed through the transwell chamber stained by crystal violet dye (10×). Data are represented as mean ± SD (n ≥ 3). \*p < 0.05, \*\*p < 0.01 vs Control group, #p < 0.05, ###p < 0.01 vs Fresh group.



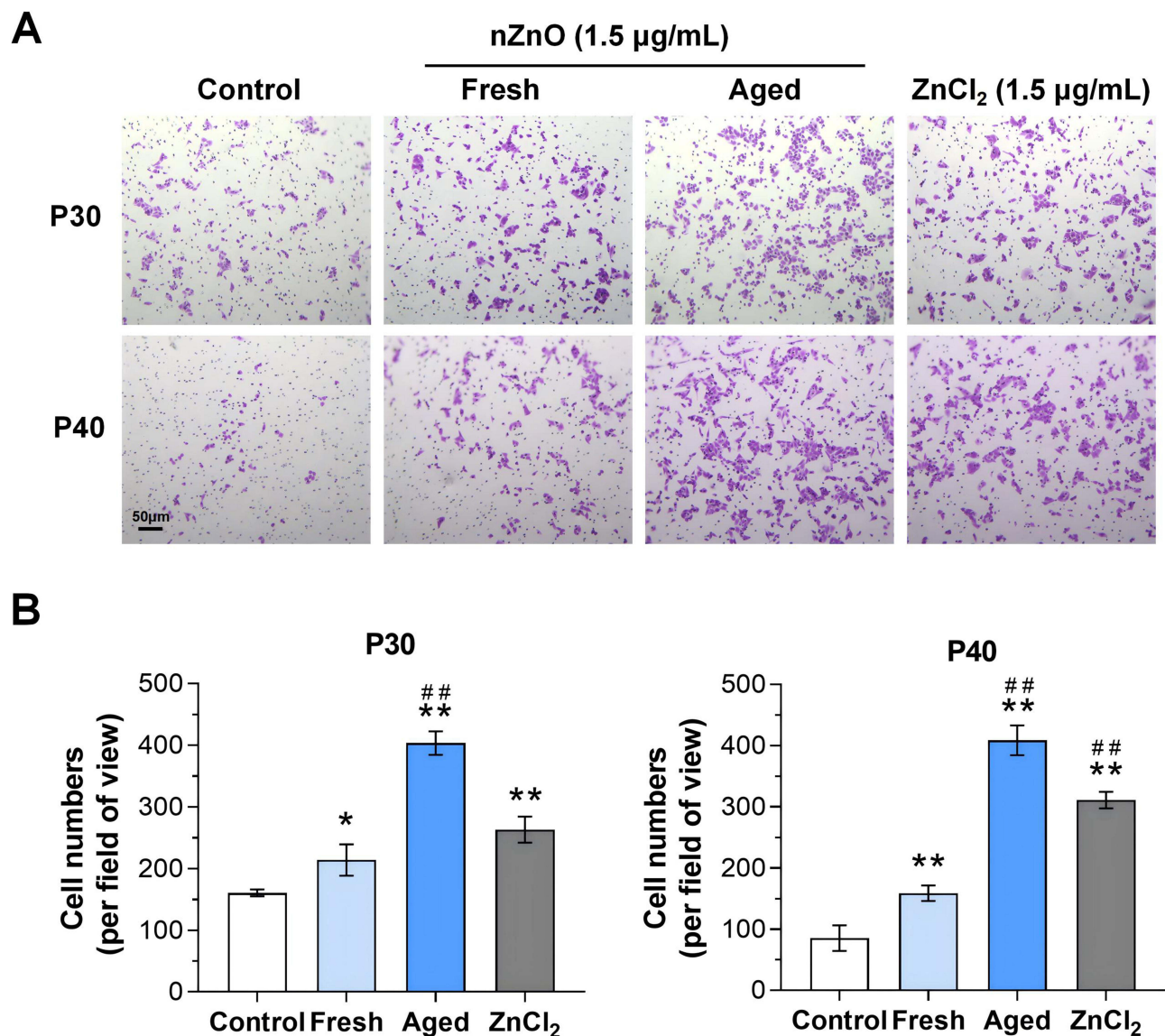


**Figure 6** Long-term exposure to low dose of nZnO increased the invasion abilities of HepG2 cells. Representative images (**A**) and the numbers (**B**) of HepG2 cells that passed through the Matrigel-Transwell chamber stained by crystal violet dye (10×). Data are represented as mean ± SD (n ≥ 3). \*p < 0.05, \*\*p < 0.01 vs Control group, ###p < 0.01 vs Fresh group.

liquids, causing oxidative stress, inflammation, and genotoxicity, and a variety of other molecular processes in cells and organisms.<sup>17,40,54,64</sup> Our previous studies also proposed that the higher cytotoxicity of fresh nZnO in the human-hamster hybrid (A<sub>L</sub>) cells could be mainly due to the intrinsic toxicity of NPs, whereas the higher mutation potential of aged nZnO might be attributed to the main contribution of Zn<sup>2+</sup> and the lesser contribution from the major transformed products, that is, Zn<sub>5</sub>(CO<sub>3</sub>)<sub>2</sub>(OH)<sub>6</sub>.<sup>40</sup> Therefore, in the present study, we used ZnCl<sub>2</sub> as a Zn<sup>2+</sup> control to elucidate the role of dissolution in the malignant progression of cancer cells promoted by nZnO. The results of the migration and invasion assays confirmed that Zn<sup>2+</sup> release is involved in the malignant progression of HepG2 cells promoted by aged NPs, although it is still not the only contributor.

## Enhanced Tumorigenicity of HepG2 Cells in vivo After Chronic Exposure to Low Dose of Aged nZnO

To further verify the promotional effect of nZnO on the tumorigenic ability of HepG2 cells in vivo, we exposed HepG2 cells to nZnO or ZnCl<sub>2</sub> for 40 passages to perform tumorigenic experiments using BALB/c nude mice. According to our

observations, tumor growth was observed in the aged and  $\text{ZnCl}_2$  groups from day 5, whereas tumor production was observed in the fresh and control groups on day 6. By day 10, the average tumor size in the aged NP-treated and  $\text{ZnCl}_2$  groups was significantly larger than that in the control group (Figure 7A–C). In addition, the weight of the tumors in the aged NP-treated- and  $\text{ZnCl}_2$ -treated groups was larger than that in the other two groups (Figure 7D). There was no significant difference in the body weights of the mice in each group throughout the process of tumor formation (Figure 7E).

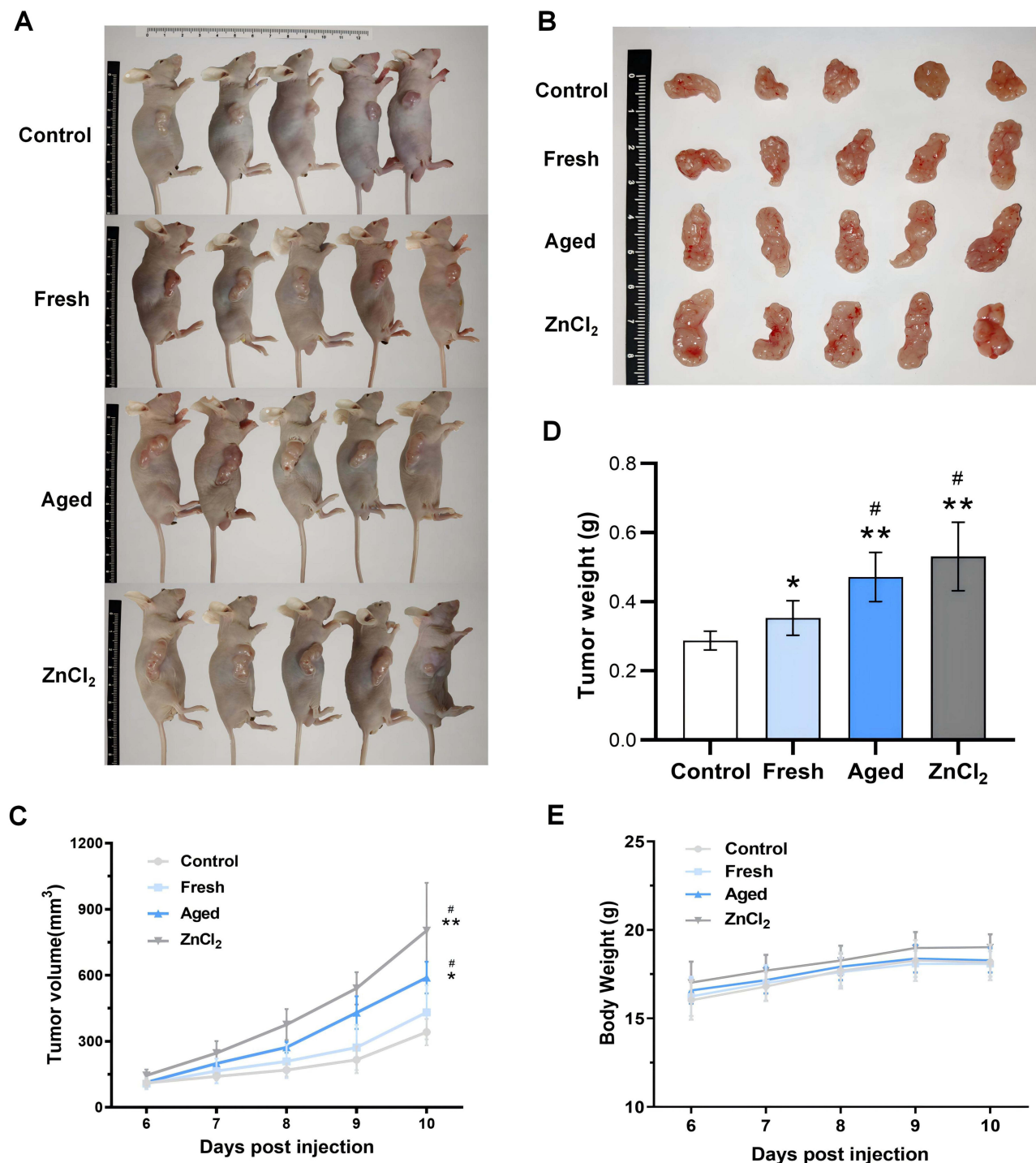


**Figure 7** Chronic exposure to nZnO promoted the tumor growth of HepG2 cells (Passage 40th) in mouse xenograft model in vivo. Representative images of animals (A) and isolated tumors (B) taken on day 10. (C) The subcutaneous tumor growth curves of 40 passages. (D) Quantification of the tumor weight. (E) The body weight of nude mice was checked everyday. Data are represented as mean  $\pm$  SD (n=5). \* $p < 0.05$ , \*\* $p < 0.01$  vs Control group; # $p < 0.05$  vs Fresh group.



Taken together, our data suggest that chronic exposure to low dose of nZnO (especially aged NPs) could promote the growth and metastasis of HepG2 cells *in vivo*, and that zinc ions could play a major role in the pro-carcinogenic effects induced by aged nZnO. In a previous *in vitro* study, we discovered that both fresh and aged nZnO promoted malignant transformation in cultured MEF cells.<sup>41</sup> Therefore, potential health risks associated with nZnO should not be overlooked. In the current study, we discovered that low dose and long-term exposure to nZnO could promote malignant progression of hepatocellular carcinoma cells. Subcutaneous and orthotopic xenograft animal models are frequently used in medical research. Subcutaneous models are reproducible and tumors become visible and are palpable. Orthotopic models replicate aspects of the cancer microenvironment and are more clinically relevant. Generally, *in situ* orthotopic models are more suitable for studying the cancer-promoting metastatic effects of pollutants than subcutaneous tumor models in nude mice.<sup>72</sup> However, considering that the *in situ* model is relatively time-consuming and the metastatic process of cancer cells is complicated, we chose the subcutaneous tumor model in the present study to initially evaluate and explore the promotional effect and mechanism of nZnO in liver cancer progression. Actually, we also investigated the potential carcinogenicity of nZnO in a wild type normal mouse model (data not shown).

## RNA-Sequencing Reveals That nZnO Exposure Upregulated CLDN2 Expression in HepG2 Cells

To gain insight into the mechanism by which aged nZnO promoted the progression of hepatocellular carcinoma cells, RNA sequencing (RNA-seq) was performed to compare the genome-wide transcriptional profiles of cells long-term treated with fresh and aged NPs, as well as ZnCl<sub>2</sub> (Figure 8A). Gene ontology (GO) enrichment analysis was performed using topGO, and the P-value was calculated using the hypergeometric distribution method (the criterion for significant enrichment was  $p < 0.05$ ) to determine the GO terms that were significantly enriched for the differentially expressed genes, and thus to identify the main biological functions exercised by the differential genes. Kyoto Encyclopedia of Genes and Genomes (KEGG) pathway enrichment analysis was performed using the clusterProfiler (3.16.1) software. Based on GO enrichment analysis, we identified biological processes associated with the malignant behavior of cells in the aged nZnO-treated group (Figure 8B), including epithelial cell proliferation, cell adhesion, regulation of cell migration, and hepatocyte proliferation. The corresponding KEGG-enriched pathways are shown in Figure 8C. Subsequently, a heat map based on the 31 upregulated genes enriched by the selected GO terms was constructed (Figure 8D). As the aforementioned assays indicated profound effects of aged nZnO on cell growth/proliferation and cell migration/metastasis (Figures 3–7), comparative intersection analysis was conducted to examine the upregulated genes in aged nZnO-treated samples, followed by validation of the expression levels of candidate genes using RT-qPCR (Figure 8E). Among all upregulated genes, we focused on claudin-2 (CLDN2), which was significantly upregulated in all three treatment groups and was further verified by Western blotting (Figure S2). CLDN2 is an integral membrane protein and a member of the tight junction protein family of proteins.<sup>43,73,74</sup> In 2009, CLDN2 was found to increase the permeability of A549 cells, and a leaky barrier may contribute to metastasis-enhancing tumor remodeling by increasing the uptake of nutrients and growth factors.<sup>75</sup> Later, a multitude of pro-proliferative and cancer-related signaling pathways was shown to affect CLDN2 abundance.<sup>76</sup> Recently, a study by Wei et al<sup>77</sup> showed that CLDN2 inhibits the expression of N-myc downstream regulated gene 1 (NDRG1) and promotes the progression of colorectal cancer by stabilizing the CLDN2/ZO1/ZONAB complex. Therefore, we speculated that CLDN2 might also play a role in the malignant progression of hepatocellular carcinoma enhanced by nZnO exposure. Compelling evidence indicates that altered CLDN2 expression affects vital biological processes, such as proliferation, migration, and cell fate decisions. These effects cannot be explained by the permeability function of CLDN2, and appear to be mediated by specific signaling pathways and transcription factors.

## Knockdown of CLDN2 Mitigated the Malignant Proliferation and Migration/Invasion of nZnO-Treated HepG2 Cells

CLDN2 has been proved to be required for the progression of various cancers through its expression aberrance.<sup>75,78–80</sup> To elucidate the underlying molecular mechanism by which CLDN2 facilitates the malignant proliferation and progression

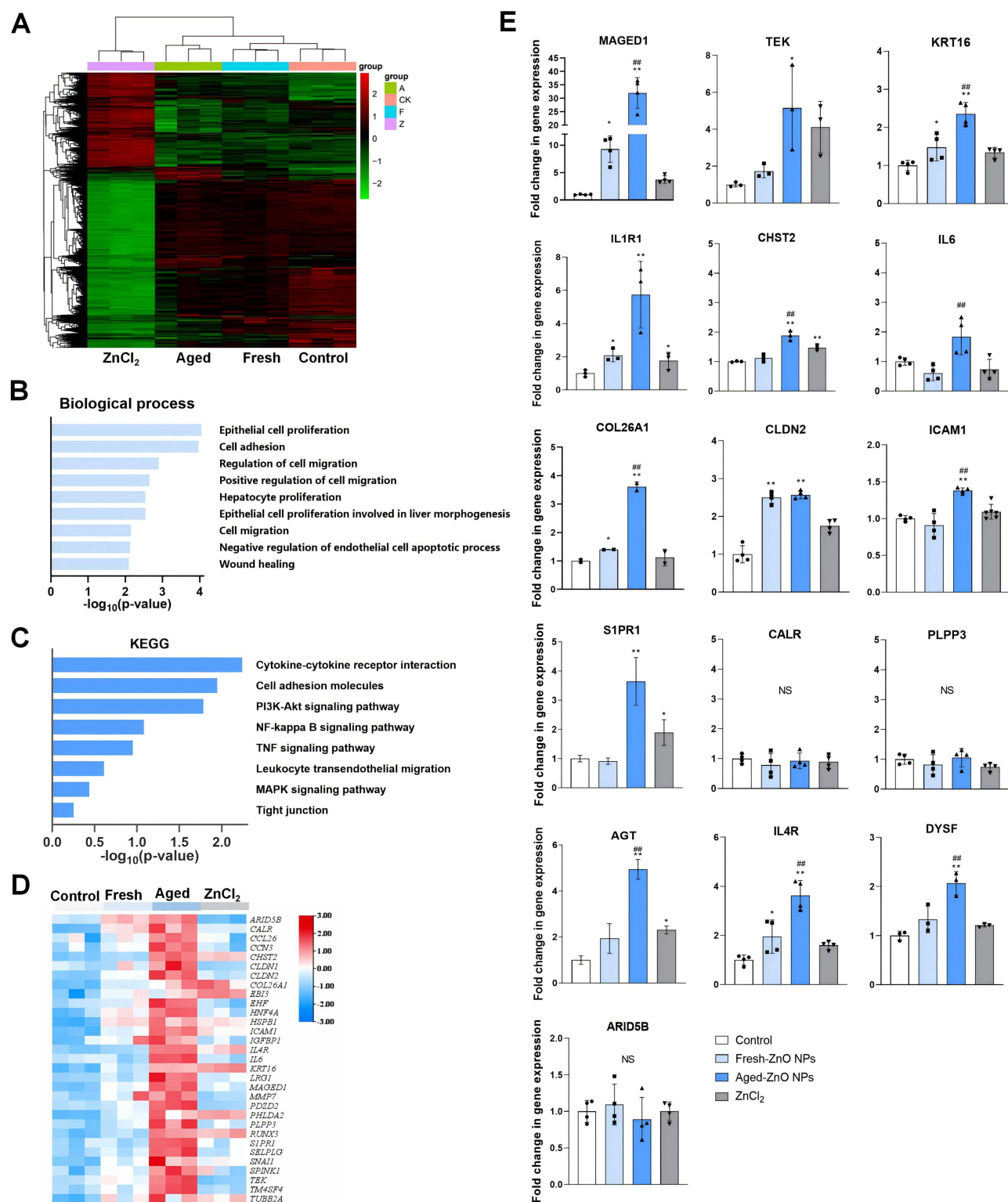


**Figure 8** Transcriptomic analysis of HepG2 cells (Passage 40<sup>th</sup>) exposed to nZnO for long-term at low dose demonstrates that CLDN2 is up-regulated in Aged groups. **(A)** RNA sequencing and cluster analysis of differentially expressed mRNAs in four groups (Control, Fresh, Aged and ZnCl<sub>2</sub>). **(B)** Enriched Biological Processes with GO term using differentially expressed genes were listed. **(C)** KEGG term. **(D)** Comparative intersection analysis of upregulated genes in aged groups. **(E)** qPCR verification based on transcriptome sequencing. Data are represented as mean  $\pm$  SD ( $n \geq 3$ ). \* $p < 0.05$ , \*\* $p < 0.01$  vs Control group, \*\*\* $p < 0.01$  vs Fresh group, NS, not significant.

of HepG2 cells induced by long-term nZnO treatment, we constructed *CLDN2* knockdown (shCLDN2#1 and shCLDN2#2) cell lines. First, we found that the number of cell colonies in nZnO-treated *CLDN2*-knockdown cells was markedly decreased, which was in contrast to that observed in nZnO-treated *CLDN2*-normal cells ([Figure S3](#)). These results suggested that high *CLDN2* expression could mediate aged nZnO-promoted cell proliferation, whereas silencing of *CLDN2* expression inhibited aged nZnO-promoted cell proliferation in HepG2 cells. The causal link between elevated *CLDN2* and cancer properties has been proven by research through the overexpression of exogenous *CLDN2* in colorectal cancer cell lines. Studies have shown that an increase in *CLDN2* expression promotes colonocyte proliferation and anchorage-independent colony formation and stimulates tumor formation in colorectal cancer xenografts and human lung adenocarcinoma cells.<sup>81–83</sup> Similarly, as shown in [Figures S4](#) and [S5](#), shCLDN2#1 and shCLDN2#2 attenuated nZnO- and ZnCl<sub>2</sub>- induced migration and invasion of *CLDN2*-normal HepG2 cells. Collectively, these results indicate that *CLDN2* may play an oncogenic role in promoting the malignant progression of human hepatoma cells triggered by nZnO, especially aged NPs. In addition, a recent study by Wei et al<sup>77</sup> showed that *CLDN2* could inhibit the expression of NDRG1 (N-myc downstream regulated gene 1) and promote the progression of colorectal cancer by stabilizing the *CLDN2*/ZO1/ZONAB complex. To further explore the mechanism of *CLDN2*'s role in the promotion of hepatocellular carcinoma cell metastasis by aged nZnO, we examined NDRG1 protein expression levels in *CLDN2*-normal and *CLDN2*-knockdown HepG2 cells chronically exposed to nZnO. As shown in [Figure S6](#), NDRG1 expression was significantly decreased in HepG2 cells chronically exposed to nZnO for up to four months. In contrast, its expression was restored in *CLDN2*-knockdown HepG2 cells, implying that *CLDN2* suppresses NDRG1 expression in HepG2 cells ([Figure S7](#)). Collectively, these results suggest that nZnO (especially aged nZnO) could possibly exert its pro-metastatic effects on HepG2 cells by inducing the upregulation of *CLDN2* expression and thus inhibiting the expression of NDRG1. Of course, this requires further experimental research and exploration. Taken together, although we did not resolve the specific mechanisms by which fresh and aged nZnO promotes tumor cell progression, our findings provide new evidence and clues for studying and comprehensively assessing the health effects of NMs on the onset and progression of cancer.

## Conclusion

Hepatocellular carcinoma is one of the most pernicious tumors that seriously harm human health. HCC metastasis is one of the primary causes of cancer treatment failure; thus, the risk factors for HCC metastasis require further investigation. As our previous findings have revealed the chemical transformations of nZnO with aging and the resulting alterations in its carcinogenicity, the present study was undertaken to evaluate the promotional effects of both fresh and aged nZnO on HCC cells. Acute exposure to a high dose of 20 nm fresh nZnO exhibited significant cytotoxicity to HepG2 cells. In comparison, we observed that aged NPs with relatively lower acute cytotoxicity could exacerbate more pronounced tumor growth and progression at the same low dose with the same long-term HepG2 cell exposure scenario as fresh NPs. The promotion of malignant progression of HepG2 cells exhibited by nZnO is associated with the activation of the cell adhesion and tight junction pathways. *CLDN2* may play a vital role in this process. Our findings suggest that the environmental transformation of NPs with aging exerts a promotion role in their oncogenic potential, providing new insights into the health risk assessment of NPs. However, further studies are needed to analyze the real state, behavior, and toxicity of NPs in the environment, as well as the cancer-promoting effects of pristine and transformed NPs in vivo, and to elucidate the cancer-promoting mechanisms of NPs.

## Acknowledgments

This work was supported in part by grants from the National Natural Science Foundation of China (22176002 and 82202489), Anhui Provincial Natural Science Foundation (2008085MB49), the Funded Project of Anhui Medical University's Research Level Improvement Program (2021xkjT004), and Anhui Provincial Undergraduate Innovation and Entrepreneurship Training Program (S202310366007 and S202310366110).

## Disclosure

The authors report no conflicts of interest in this work.

## References

- Zhan QR, Liu BX, Situ XH, et al. New insights into the correlations between circulating tumor cells and target organ metastasis. *Signal Transduct Target Ther*. 2023;8(1):465. doi:10.1038/s41392-023-01725-9
- Jin X, Demere Z, Nair K, et al. A metastasis map of human cancer cell lines. *Nature*. 2020;588(7837):331–336. doi:10.1038/s41586-020-2969-2
- Peng F, Setyawati MI, Tee JK, et al. Nanoparticles promote *in vivo* breast cancer cell intravasation and extravasation by inducing endothelial leakiness. *Nat Nanotechnol*. 2019;14(3):279–286. doi:10.1038/s41565-018-0356-z
- Chen SM, Cao Z, Prettnner K, et al. Estimates and projections of the global economic cost of 29 cancers in 204 countries and territories from 2020 to 2050. *JAMA Oncol*. 2023;9(4):465–472. doi:10.1001/jamaoncol.2022.7826
- Wu HT, Eckhardt CM, Baccarelli AA. Molecular mechanisms of environmental exposures and human disease. *Nat Rev Genet*. 2023;24(5):332–344. doi:10.1038/s41576-022-00569-3
- National Cancer Institute. Cancer-causing substances in the environment. Available from: <https://www.cancer.gov/about-cancer/causes-prevention/risk/substances>. Accessed January 5, 2024.
- Setyawati MI, Sevensan C, Bay BH, et al. Nano-TiO<sub>2</sub> drives epithelial-mesenchymal transition in intestinal epithelial cancer cells. *Small*. 2018;14(30):e1800922. doi:10.1002/sml.201800922
- Zhu S, Li LL, Gu ZJ, Chen CY, Zhao YL. 15 years of small: research trends in nanosafety. *Small*. 2020;16(36):e2000980. doi:10.1002/sml.202000980
- Meng J, Yang J, Pan T, Qu XJ, Cui SX. ZnO nanoparticles promote the malignant transformation of colorectal epithelial cells in APC<sup>min/+</sup> mice. *Environ Int*. 2022;158:106923. doi:10.1016/j.envint.2021.106923
- Li YJ, Li FX, Zhang LC, et al. Zinc oxide nanoparticles induce mitochondrial biogenesis impairment and cardiac dysfunction in human iPSC-derived cardiomyocytes. *Int J Nanomed*. 2020;15:2669–2683. doi:10.2147/IJN.S249912
- Keller AA, McFerran S, Lazareva A, Suh S. Global life cycle releases of engineered nanomaterials. *J Nanopart Res*. 2013;15(6):1692. doi:10.1007/s11051-013-1692-4
- Barguilla I, Barszczewska G, Annangi B, et al. MTH1 is involved in the toxic and carcinogenic long-term effects induced by zinc oxide and cobalt nanoparticles. *Arch Toxicol*. 2020;94(6):1973–1984. doi:10.1007/s00204-020-02737-y
- Makvandi P, Wang CY, Zare EN, Borzacchiello A, Niu LN, Tay FR. Metal-based nanomaterials in biomedical applications: antimicrobial activity and cytotoxicity aspects. *Adv Funct Mater*. 2020;30:22. doi:10.1002/adfm.201910021
- Sohail MI, Waris AA, Ayub MA, et al. Environmental application of nanomaterials: a promise to sustainable future. *Compr Anal Chem*. 2019;87:1–54. doi:10.1016/bs.coac.2019.10.002
- McClements DJ, Xiao H. Is nano safe in foods? Establishing the factors impacting the gastrointestinal fate and toxicity of organic and inorganic food-grade nanoparticles. *NPJ Sci Food*. 2017;1:6. doi:10.1038/s41538-017-0005-1
- Vallabani NVS, Sengupta S, Shukla RK, Kumar A. ZnO nanoparticles-associated mitochondrial stress-induced apoptosis and G2/M arrest in HaCaT cells: a mechanistic approach. *Mutagenesis*. 2019;34(3):265–277. doi:10.1093/mutage/gez017
- Wang MM, Wang J, Liu Y, et al. Subcellular targets of zinc oxide nanoparticles during the aging process: role of cross-talk between mitochondrial dysfunction and endoplasmic reticulum stress in the genotoxic response. *Toxicol Sci*. 2019a;171(1):159–171. doi:10.1093/toxsci/kfz132
- Park EJ, Jeong U, Yoon C, Kim Y. Comparison of distribution and toxicity of different types of zinc-based nanoparticles. *Environ Toxicol*. 2017;32(4):1363–1374. doi:10.1002/tox.22330
- Pati R, Das I, Mehta RK, Sahu R, Sonawane A. Zinc-oxide nanoparticles exhibit genotoxic, clastogenic, cytotoxic and actin depolymerization effects by inducing oxidative stress responses in macrophages and adult mice. *Toxicol Sci*. 2016;150(2):454–472. doi:10.1093/toxsci/kfw010
- Yu J, Choi SJ. Particle size and biological fate of ZnO do not cause acute toxicity, but affect toxicokinetics and gene expression profiles in the rat livers after oral administration. *Int J Mol Sci*. 2021;22(4):1698. doi:10.3390/ijms22041698
- Li JL, Chen CY, Xia T. Understanding nanomaterial-liver interactions to facilitate the development of safer nanoapplications. *Adv Mater*. 2022;34(11):e2106456. doi:10.1002/adma.202106456
- Kielbik P, Kaszewski J, Rosowska J, et al. Biodegradation of the ZnO:Eu nanoparticles in the tissues of adult mouse after alimentary application. *Nanomedicine*. 2017;13(3):843–852. doi:10.1016/j.nano.2016.11.002
- Kuang HJ, Yang PF, Yang L, Aguilar ZP, Xu HY. Size dependent effect of ZnO nanoparticles on endoplasmic reticulum stress signaling pathway in murine liver. *J Hazard Mater*. 2016;317:119–126. doi:10.1016/j.jhazmat.2016.05.063
- Wang C, Lu J, Zhou L, et al. Effects of long-term exposure to zinc oxide nanoparticles on development, zinc metabolism and biodistribution of minerals (Zn, Fe, Cu, Mn) in Mice. *PLoS One*. 2016;11(10):e0164434. doi:10.1371/journal.pone.0164434
- Chen AJ, Feng XL, Sun T, Zhang YL, An SL, Shao LQ. Evaluation of the effect of time on the distribution of zinc oxide nanoparticles in tissues of rats and mice: a systematic review. *IET Nanobiotechnol*. 2016;10(3):97–106. doi:10.1049/iet-nbt.2015.0006
- Baek M, Chung HE, Yu J, et al. Pharmacokinetics, tissue distribution, and excretion of zinc oxide nanoparticles. *Int J Nanomed*. 2012;7:3081–3097. doi:10.2147/IJN.S32593
- Park HS, Shin SS, Meang EH, et al. A 90-day study of subchronic oral toxicity of 20 nm, negatively charged zinc oxide nanoparticles in Sprague Dawley rats. *Int J Nanomed*. 2014;9(Suppl 2):79–92. doi:10.2147/IJN.S57926
- Watson CY, Molina RM, Louzada A, Murdaugh KM, Donaghey TC, Brain JD. Effects of zinc oxide nanoparticles on Kupffer cell phagosomal motility, bacterial clearance, and liver function. *Int J Nanomed*. 2015;10:4173–4184. doi:10.2147/IJN.S82807
- Kermanizadeh A, Jantzen K, Ward MB, et al. Nanomaterial-induced cell death in pulmonary and hepatic cells following exposure to three different metallic materials: the role of autophagy and apoptosis. *Nanotoxicology*. 2017;11(2):184–200. doi:10.1080/17435390.2017.1279359
- Kermanizadeh A, Lohr M, Roursgaard M, et al. Hepatic toxicology following single and multiple exposure of engineered nanomaterials utilising a novel primary human 3D liver microtissue model. *Part Fibre Toxicol*. 2014;11:56. doi:10.1186/s12989-014-0056-2
- Kong T, Zhang SH, Zhang C, et al. Long-term effects of unmodified 50 nm ZnO in mice. *Biol Trace Elem Res*. 2019;189(2):478–489. doi:10.1007/s12011-018-1477-9
- Agents classified by the IARC monographs, volumes 1–128. Available from: <https://monographs.iarc.who.int/list-of-classifications/>. Accessed January 30, 2024.



33. Lu XF, Zhu Y, Bai R, et al. Long-term pulmonary exposure to multi-walled carbon nanotubes promotes breast cancer metastatic cascades. *Nat Nanotechnol.* **2019**;14(7):719–727. doi:10.1038/s41565-019-0472-4
34. Gomez-Gonzalez MA, Koronfel MA, Pullin H, et al. Nanoscale chemical imaging of nanoparticles under real-world wastewater treatment conditions. *Adv Sustain Syst.* **2021**;5:2100023. doi:10.1002/adsu.202100023
35. Clar JG, Platten WE III, Baumann E, et al. Release and transformation of ZnO nanoparticles used in outdoor surface coatings for UV protection. *Sci Total Environ.* **2019**;670:78–86. doi:10.1016/j.scitotenv.2019.03.189
36. Bundschuh M, Filser J, Lüderwald S, et al. Nanoparticles in the environment: where do we come from, where do we go to? *Environ Sci Eur.* **2018**;30(1):6. doi:10.1186/s12302-018-0132-6
37. Zhang HZ, Gilbert B, Huang F, Banfield JF. Water-driven structure transformation in nanoparticles at room temperature. *Nature.* **2003**;424(6952):1025–1029. doi:10.1038/nature01845
38. Spurgeon DJ, Lahive E, Schultz CL. Nanomaterial transformations in the environment: effects of changing exposure forms on bioaccumulation and toxicity. *Small.* **2020**;16(36):e2000618. doi:10.1002/smll.202000618
39. Wigger H, Kägi R, Wiesner M, Nowack B. Exposure and possible risks of engineered nanomaterials in the environment—current knowledge and directions for the future. *Rev Geophys.* **2020**;58. doi:10.1029/2020RG000710
40. Wang MM, Wang YC, Wang XN, et al. Mutagenicity of ZnO nanoparticles in mammalian cells: role of physicochemical transformations under the aging process. *Nanotoxicology.* **2015**;9(8):972–982. doi:10.3109/17435390.2014.992816
41. Wang MM, Cao R, Jiang WG, et al. Long-term exposure to low doses of fresh and aged zinc oxide nanoparticles causes cell malignant progression enhanced by a tyrosine phosphatase SHP2 gain-of-function mutation. *Environ Sci-Nano.* **2019b**. doi:10.1039/C8EN01191E
42. Uzhytchak M, Lunova M, Smolková B, Jirsa M, Dejneka A, Lunov O. Iron oxide nanoparticles trigger endoplasmic reticulum damage in steatotic hepatic cells. *Nanoscale Adv.* **2023**;5(16):4250–4268. doi:10.1039/d3na00071k
43. Hashimoto Y, Hata T, Tada M, et al. Safety evaluation of a human chimeric monoclonal antibody that recognizes the extracellular loop domain of claudin-2. *Eur J Pharm Sci.* **2018**;117:161–167. doi:10.1016/j.ejps.2018.02.016
44. George S, Pokhrel S, Xia T, et al. Use of a rapid cytotoxicity screening approach to engineer a safer zinc oxide nanoparticle through iron doping. *ACS Nano.* **2010**;4(1):15–29. doi:10.1021/nn901503q
45. Zhang J, Guo WL, Li QQ, Wang Z, Liu SJ. The effects and the potential mechanism of environmental transformation of metal nanoparticles on their toxicity in organisms. *Environ Sci-Nano.* **2018**;5:2482–2499. doi:10.1039/C8EN00688A
46. Mitrano DM, Motellier S, Clavaguera S, Nowack B. Review of nanomaterial aging and transformations through the life cycle of nano-enhanced products. *Environ Int.* **2015**;77:132–147. doi:10.1016/j.envint.2015.01.013
47. Sivry Y, Gelabert A, Cordier L, et al. Behavior and fate of industrial zinc oxide nanoparticles in a carbonate-rich river water. *Chemosphere.* **2014**;95:519–526. doi:10.1016/j.chemosphere.2013.09.110
48. Reed RB, Ladner DA, Higgins CP, Westerhoff P, Ranville JF. Solubility of nano-zinc oxide in environmentally and biologically important matrices. *Environ Toxicol Chem.* **2012**;31(1):93–99. doi:10.1002/etc.708
49. Lowry GV, Gregory KB, Apte SC, Lead JR. Transformations of nanomaterials in the environment. *Environ Sci Technol.* **2012**;46(13):6893–6899. doi:10.1021/es300839e
50. Scheckel KG, Luxton TP, El Badawy AM, Impellitteri CA, Tolaymat TM. Synchrotron speciation of silver and zinc oxide nanoparticles aged in a kaolin suspension. *Environ Sci Technol.* **2010**;44(4):1307–1312. doi:10.1021/es9032265
51. Lombi E, Donner E, Tavakkoli E, et al. Fate of zinc oxide nanoparticles during anaerobic digestion of wastewater and post-treatment processing of sewage sludge. *Environ Sci Technol.* **2012**;46(16):9089–9096. doi:10.1021/es301487s
52. Ma R, Levard C, Judy JD, et al. Fate of zinc oxide and silver nanoparticles in a pilot wastewater treatment plant and in processed biosolids. *Environ Sci Technol.* **2014**;48(1):104–112. doi:10.1021/es403646x
53. Sharma V, Singh P, Pandey AK, Dhawan A. Induction of oxidative stress, DNA damage and apoptosis in mouse liver after sub-acute oral exposure to zinc oxide nanoparticles. *Mutat Res.* **2012**;745(1–2):84–91. doi:10.1016/j.mrgentox.2011.12.009
54. Liu J, Feng X, Wei L, Chen L, Song B, Shao L. The toxicology of ion-shedding zinc oxide nanoparticles. *Crit Rev Toxicol.* **2016**;46(4):348–384. doi:10.3109/10408444.2015.1137864
55. Anand AS, Jain K, Chauhan A, Prasad DN, Kohli E. Zinc oxide nanoparticles trigger dysfunction of mitochondrial respiratory complexes and repair dynamics in human alveolar cells. *Toxicol Ind Health.* **2023**;39(3):127–137. doi:10.1177/07482337231152956
56. Li Y, Zhang Y, Yan B. Nanotoxicity overview: nano-threat to susceptible populations. *Int J Mol Sci.* **2014**;15(3):3671–3697. doi:10.3390/ijms15033671
57. Yan DJ, Long JM, Liu JK, Cao Y. The toxicity of ZnO nanomaterials to HepG2 cells: the influence of size and shape of particles. *J Appl Toxicol.* **2019**;39(2):231–240. doi:10.1002/jat.3712
58. Chen PY, Wang H, He M, Chen BB, Yang B, Hu B. Size-dependent cytotoxicity study of ZnO nanoparticles in HepG2 cells. *Ecotoxicol Environ Saf.* **2019**;171:337–346. doi:10.1016/j.ecoenv.2018.12.096
59. Zhang H, Huang Q, Xu A, Wu LJ. Spectroscopic probe to contribution of physicochemical transformations in the toxicity of aged ZnO NPs to *Chlorella vulgaris*: new insight into the variation of toxicity of ZnO NPs under aging process. *Nanotoxicology.* **2016**;10(8):1177–1187. doi:10.1080/17435390.2016.1196252
60. Li M, Lin DH, Zhu LZ. Effects of water chemistry on the dissolution of ZnO nanoparticles and their toxicity to *Escherichia coli*. *Environ Pollut.* **2013**;173:97–102. doi:10.1016/j.envpol.2012.10.026
61. Vandebriel RJ, De Jong WH. A review of mammalian toxicity of ZnO nanoparticles. *Nanotechnol Sci Appl.* **2012**;5:61–71. doi:10.2147/NSA.S23932
62. Franklin NM, Rogers NJ, Apte SC, Batley GE, Gadd GE, Casey PS. Comparative toxicity of nanoparticulate ZnO, bulk ZnO, and ZnCl<sub>2</sub> to a freshwater microalga (*Pseudokirchneriella subcapitata*): the importance of particle solubility. *Environ Sci Technol.* **2007**;41(24):8484–8490. doi:10.1021/es071445r
63. Demir E, Akça H, Kaya B, et al. Zinc oxide nanoparticles: genotoxicity, interactions with UV-light and cell-transforming potential. *J Hazard Mater.* **2014**;264:420–429. doi:10.1016/j.jhazmat.2013.11.043
64. James SA, Feltis BN, de Jonge MD, et al. Quantification of ZnO nanoparticle uptake, distribution, and dissolution within individual human macrophages. *ACS Nano.* **2013**;7(12):10621–10635. doi:10.1021/nn403118u



65. Song WH, Zhang JY, Guo J, et al. Role of the dissolved zinc ion and reactive oxygen species in cytotoxicity of ZnO nanoparticles. *Toxicol Lett.* 2010;199(3):389–397. doi:10.1016/j.toxlet.2010.10.003
66. Zhang CP, Liu ZX, Zhang YH, Ma L, Song E, Song Y. "Iron free" zinc oxide nanoparticles with ion-leaking properties disrupt intracellular ROS and iron homeostasis to induce ferroptosis. *Cell Death Dis.* 2020;11(3):183. doi:10.1038/s41419-020-2384-5
67. Raghupathi KR, Koodali RT, Manna AC. Size-dependent bacterial growth inhibition and mechanism of antibacterial activity of zinc oxide nanoparticles. *Langmuir.* 2011;27(7):4020–4028. doi:10.1021/la104825u
68. Vales G, Rubio L, Marcos R. Genotoxic and cell-transformation effects of multi-walled carbon nanotubes (MWCNT) following in vitro sub-chronic exposures. *J Hazard Mater.* 2016;306:193–202. doi:10.1016/j.jhazmat.2015.12.021
69. Vila L, Marcos R, Hernández A. Long-term effects of silver nanoparticles in caco-2 cells. *Nanotoxicology.* 2017;11(6):771–780. doi:10.1080/17435390.2017.1355997
70. Annangi B, Rubio L, Alaraby M, Bach J, Marcos R, Hernández A. Acute and long-term in vitro effects of zinc oxide nanoparticles. *Arch Toxicol.* 2016;90(9):2201–2213. doi:10.1007/s00204-015-1613-7
71. Kushwaha PP, Gupta S, Singh AK, Kumar S. Emerging role of migration and invasion enhancer 1 (MIEN1) in cancer progression and metastasis. *Front Oncol.* 2019;9:868. doi:10.3389/fonc.2019.00868
72. Cai KX, Tse LY, Leung C, Tam PK, Xu R, Sham MH. Suppression of lung tumor growth and metastasis in mice by adeno-associated virus-mediated expression of vasostatin. *Clin Cancer Res.* 2008;14(3):939–949. doi:10.1158/1078-0432.CCR-07-1930
73. Takigawa M, Iida M, Nagase S, et al. Creation of a Claudin-2 binder and its tight junction-modulating activity in a human intestinal model. *J Pharmacol Exp Ther.* 2017;363(3):444–451. doi:10.1124/jpet.117.242214
74. Furuse M, Fujita K, Hiiiragi T, Fujimoto K, Tsukita S. Claudin-1 and -2: novel integral membrane proteins localizing at tight junctions with no sequence similarity to occludin. *J Cell Biol.* 1998;141(7):1539–1550. doi:10.1083/jcb.141.7.1539
75. Peter Y, Comellas A, Levantini E, Ingenito EP, Shapiro SD. Epidermal growth factor receptor and claudin-2 participate in A549 permeability and remodeling: implications for non-small cell lung cancer tumor colonization. *Mol Carcinog.* 2009;48(6):488–497. doi:10.1002/mc.20485
76. Venugopal S, Anwer S, Szász K. Claudin-2: roles beyond permeability functions. *Int J Mol Sci.* 2019;20(22):5655. doi:10.3390/ijms20225655
77. Wei MT, Zhang YG, Yang XY, et al. Claudin-2 promotes colorectal cancer growth and metastasis by suppressing NDRG1 transcription. *Clin Transl Med.* 2021;11(12):e667. doi:10.1002/ctm2.667
78. Tabariès S, Dong Z, Annis MG, et al. Claudin-2 is selectively enriched in and promotes the formation of breast cancer liver metastases through engagement of integrin complexes. *Oncogene.* 2011;30(11):1318–1328. doi:10.1038/onc.2010.518
79. Tabariès S, McNulty A, Ouellet V, et al. Afadin cooperates with Claudin-2 to promote breast cancer metastasis. *Genes Dev.* 2019;33(3–4):180–193. doi:10.1101/gad.319194.118
80. Buchert M, Papin M, Bonnans C, et al. Symplekin promotes tumorigenicity by up-regulating claudin-2 expression. *Proc Natl Acad Sci U S A.* 2010;107(6):2628–2633. doi:10.1073/pnas.0903747107
81. Dhawan P, Ahmad R, Chaturvedi R, et al. Claudin-2 expression increases tumorigenicity of colon cancer cells: role of epidermal growth factor receptor activation. *Oncogene.* 2011;30(29):3234–3247. doi:10.1038/onc.2011.43
82. Ahmad R, Chaturvedi R, Olivares-Villagómez D, et al. Targeted colonic claudin-2 expression renders resistance to epithelial injury, induces immune suppression, and protects from colitis. *Mucosal Immunol.* 2014;7(6):1340–1353. doi:10.1038/mi.2014.21
83. Ikari A, Watanabe R, Sato T, et al. Nuclear distribution of claudin-2 increases cell proliferation in human lung adenocarcinoma cells. *Biochim Biophys Acta.* 2014;1843(9):2079–2088. doi:10.1016/j.bbamcr.2014.05.017

## International Journal of Nanomedicine

Dovepress

### Publish your work in this journal

The International Journal of Nanomedicine is an international, peer-reviewed journal focusing on the application of nanotechnology in diagnostics, therapeutics, and drug delivery systems throughout the biomedical field. This journal is indexed on PubMed Central, MedLine, CAS, SciSearch®, Current Contents®/Clinical Medicine, Journal Citation Reports/Science Edition, EMBase, Scopus and the Elsevier Bibliographic databases. The manuscript management system is completely online and includes a very quick and fair peer-review system, which is all easy to use. Visit <http://www.dovepress.com/testimonials.php> to read real quotes from published authors.

Submit your manuscript here: <https://www.dovepress.com/international-journal-of-nanomedicine-journal>